The method of images in shear flow

By M. B. GLAUERT
Department of Mathematics, University of Manchester

(Received 20 May 1960)

The method of images is used to determine the flow perturbation caused by a small point source of fluid in a stream containing a vortex sheet, a number of vortex sheets, or a continuous two-dimensional distribution of vorticity. Calculations are carried out for a variety of such shear flows, to illustrate the range of applicability of the method.

The image source distribution provides an alternative approach to that given by Lighthill for calculating small disturbances to a parallel shear flow, and suggests a simple physical picture by which to interpret the complicated effects associated with the distortion and stretching of vortex lines.

1. Introduction

Much attention has recently been paid to the problem of calculating the effect of disturbances to a non-uniform stream of fluid containing vorticity. The flow is assumed to be steady and incompressible and viscous effects are neglected. The purely two-dimensional case is relatively simple, since the vortex lines remain straight and unstretched, but for three-dimensional disturbances the distortion of the vortex lines creates problems of an entirely different order of difficulty, even if the undisturbed stream is two-dimensional.

One approach has been to consider that the vorticity is small, and that its effect may be represented as a 'secondary flow' produced by the convection of the vorticity by the 'primary flow', that which would occur if stream vorticity were absent. Earlier work on these lines has been extended by Lighthill (1956, 1957*a*, *b*) by making use of the concept of the 'drift' of material fluid surfaces, discussed by Darwin (1953).

A second approach is to study small three-dimensional disturbances to a two-dimensional parallel stream or shear layer, without making any assumption that the stream vorticity is small. Lighthill (1957*c*) has examined the fundamental disturbance solution, that due to a small point source, and has shown that an equation for the velocity perturbation may be obtained by taking the Hankel transform of the Orr–Sommerfeld equation which governs small inviscid disturbances to the shear flow. The effects of more complicated small disturbances may be found by suitably differentiating and superposing such fundamental solutions. A basic assumption is that the source causes only a small proportionate change in velocity, and consequently the method cannot be applied for shear layers in which the stream velocity falls to zero at any finite point. Lighthill gives a very full account of the background to the problem, and obtains a great deal of valuable information about the solutions of his equation in various cases. In particular he shows that difficulties as to the nature of secondary flow solutions can be resolved by matching the secondary flow at large distance from an obstacle to the form of the small-disturbance solution at small distance.

This paper describes an alternative theory to Lighthill's for deriving the perturbation due to a small source. The shear layer is replaced by a number of layers of uniform flow, separated by vortex sheets. It is shown that the effect of the vortex sheets can be represented by a series of image sources, and that when the number of sheets tends to infinity and their spacing tends to zero a continuous image source distribution is obtained, applicable to the continuous shear layer. The restrictions on the validity of the equations are precisely the same as in Lighthill's approach, and the majority of the chief deductions of each method of analysis can be obtained by the other, in complete accord with one another in all cases.

However, the development of this alternative theory justifies itself on a number of grounds. Each of the theories may serve to stimulate development in the other, and there are important results on each side which have not yet been proved by means of the rival theory. In addition, the image system is helpful in indicating a simple physical model of the flow in a disturbed shear layer. It is not easy to visualize in detail the effect of the stretching and bending of vortex lines, and meditating on the image source distribution may lead to a better understanding of phenomena for which untutored physical intuition provides no clear guide.

2. Single vortex sheet

Consider an unbounded volume of homogeneous incompressible fluid such that, with Cartesian co-ordinates (x, y, z), the fluid in $y > 0$ (the upper region) has uniform velocity U_1 in the x-direction and in $y < 0$ (the lower region) has uniform velocity U_0 in the same direction. Thus $y = 0$ is a vortex sheet of strength $U_1 - U_0$. Suppose that there is a three-dimensional point source of fluid of small strength M at the point O in the lower region, at a distance h from the interface. Let us try to find the effect of this source by use of the method of images.

We postulate that the flow perturbation in the lower fluid is that due to M itself together with a source m_i (i for image) at O_1, the mirror image of O in the interface $y = 0$, and that the perturbation in the upper fluid is that due to a source m_t (t for transmitted) at O. There can of course be no source at O_1 for the flow in the upper region, since there is no actual singularity at this point. This representation will be legitimate only if the necessary conditions at the interface can be satisfied by a suitable choice of the values of m_i and m_t. These conditions are that the pressure shall be continuous, and that continuity shall be satisfied, which requires that the displacement of the interface in the y-direction be the same in the two regions.

Let the perturbation velocity at (x, y, z) be (u, v, w) and suppose that the source M is so small that on the interface squares and products of u, v and w may be neglected. Then by Bernoulli's equation the first of our conditions requires that over the interface, for equal increments of pressure in the two regions, $U_0 u_0 = U_1 u_1$, where the suffixes 0 and 1 indicate the lower and upper regions respectively. For small disturbances this condition may be applied on $y = 0$, the undisturbed interface, and it is satisfied by our image source distribution provided that

$$U_0(M+m_i) = U_1 m_t. \tag{2.1}$$

At a fixed position the displacement of a streamline due to a small source is inversely proportional to the stream velocity, and hence our second condition is satisfied if

$$\frac{M-m_i}{U_0} = \frac{m_t}{U_1}. \tag{2.2}$$

An alternative method of obtaining (2.2) is to interpret the continuity condition as requiring that the flow directions in the upper and lower fluids shall be compatible at the interface, and so v/U must be continuous.

From equations (2.1) and (2.2) we obtain

$$m_i = \left(\frac{U_1^2-U_0^2}{U_1^2+U_0^2}\right)M, \quad m_t = \left(\frac{2U_1U_0}{U_1^2+U_0^2}\right)M. \tag{2.3}$$

Certain special forms of these expressions are of interest. For a free surface at $y = 0$, $U_1 = 0$ and we have

$$m_i = -M, \quad m_t = 0. \tag{2.4}$$

This is a familiar result, used in the theory of wind-tunnel interference. The case of a solid boundary at $y = 0$ is obtained by putting $U_1 = \infty$, since the upper fluid then has infinite momentum and so no displacement of the interface can occur. We then have

$$m_i = M, \quad m_t = 0. \tag{2.5}$$

This value of m_i is well known from the elementary theory of the method of images, and is valid no matter how large the value of M.

An immediate practical application of the type of analysis we have been using concerns the effect at large distance of a small point source M at the origin in a shear layer of limited width. Suppose that the stream velocity varies from U_{-1} to U_1, the stream velocity at the level of the source being U_0. For numerically large values of y the shear layer may be treated as a single vortex sheet. Above the layer the flow perturbation is that due to a source m_1, and below the layer that due to a source m_{-1}, each source being at the origin. As in (2.1), pressure continuity along the vortex sheet requires

$$m_1 U_1 = m_{-1} U_{-1}. \tag{2.6}$$

The fluid from the source flows downstream to form a tube of cross-sectional area M/U_0, and displaces the surrounding stream surfaces outwards by this amount. Equating this to the displacements in the upper and lower fluids due to the effective sources, we have

$$\frac{M}{U_0} = \frac{m_1}{2U_1} + \frac{m_{-1}}{2U_{-1}}, \tag{2.7}$$

since in each case only half the flux from the source enters the appropriate region. This equation takes the place of (2.2). From equations (2.6) and (2.7) we obtain

$$m_1 = \frac{2U_1U_{-1}^2}{U_0(U_1^2+U_{-1}^2)}M, \quad m_{-1} = \frac{2U_1^2U_{-1}}{U_0(U_1^2+U_{-1}^2)}M. \tag{2.8}$$

By use of his Hankel transform method, Lighthill (1957*c*) obtained the same result, though with greater labour, and he also found the effective displacements of the sources m_1 and m_{-1} from the plane $y = 0$. The present analysis, which was briefly mentioned by Lighthill, has no obvious extension which would enable these displacements to be calculated.

3. Multiple vortex sheets

We now consider a flow in which there are a number of vortex sheets in planes y = constant, separating layers in each of which there is a uniform stream in the x-direction. By taking the vortex sheets to be sufficiently numerous and closely spaced we shall then be able to deduce results applicable to a shear flow, with continuously varying velocity.

Assume that the vortex sheets are spaced at equal intervals δ and that the perturbing source M, at $y = 0$, is at a point midway between two of the sheets. Let U_r be the stream velocity in the rth layer, with centre at $y = r\delta$. In this rth layer, we shall seek to represent the flow perturbation as that due to a set of image sources $m_{r,s}$, $s = 0, \pm 1, \pm 2, \ldots$, where s indicates the layer in the centre of which the image is located, all the images being on the line in the y-direction through the source M.

The conditions which must be satisfied at the interface between the rth and $(r+1)$th layers are that the pressure perturbation and the interface deflexion shall be consistent on the two sides, precisely as for equations (2.1) and (2.2). Furthermore, since sources at different distances produce effects which vary in different manners over the interface, the set of sources at each particular distance must satisfy the conditions separately. Thus for the sources at a distance $(k-\frac{1}{2})\,\delta$ from the interface we require

$$U_r(m_{r,r+k} + m_{r,r-k+1}) = U_{r+1}(m_{r+1,r+k} + m_{r+1,r-k+1}), \tag{3.1}$$

$$\frac{1}{U_r}(m_{r,r+k} - m_{r,r-k+1}) = \frac{1}{U_{r+1}}(m_{r+1,r+k} - m_{r+1,r-k+1}). \tag{3.2}$$

Eliminating $m_{r+1,r-k+1}$ and $m_{r,r+k}$, respectively, we may replace (3.1) and (3.2) by the equivalent pair of equations

$$(U_{r+1}^2 + U_r^2)\, m_{r,r+k} = (U_{r+1}^2 - U_r^2)\, m_{r,r-k+1} + 2U_{r+1}U_r m_{r+1,r+k}, \tag{3.3}$$

$$(U_{r+1}^2 + U_r^2)\, m_{r+1,r-k+1} = 2U_{r+1}U_r m_{r,r-k+1} - (U_{r+1}^2 - U_r^2)\, m_{r+1,r+k}. \tag{3.4}$$

In addition, from the known presence or absence of sources in the layers themselves,

$$m_{0,0} = M, \quad \text{and} \quad m_{r,r} = 0 \quad (r \neq 0). \tag{3.5}$$

Equation (3.5) gives the terms of the array $m_{r,s}$ on the principal diagonal, and in equations (3.3) and (3.4) the terms on the right are $(k-1)$ steps from the principal diagonal while the terms on the left are k steps away. Hence the calculation of the terms $m_{r,s}$ may be carried stage-by-stage away from the principal diagonal, by taking successively $k = 1, 2, 3, \ldots$.

It is possible to obtain a relation between four neighbouring image sources by elimination between (3.3) and the forms of equations (3.3) and (3.4) with r replaced by $r-1$ and k by $k-1$. The result is

$$\frac{2U_r U_{r-1}}{U_r^2 - U_{r-1}^2} m_{r-1,s-1} + \frac{2U_{r+1} U_r}{U_{r+1}^2 - U_r^2} m_{r+1,s+1} = \frac{U_r^2 + U_{r-1}^2}{U_r^2 - U_{r-1}^2} m_{r,s-1} + \frac{U_{r+1}^2 + U_r^2}{U_{r+1}^2 - U_r^2} m_{r,s+1}. \tag{3.6}$$

This equation may also be used to calculate successively the sources $m_{r,s}$.

Certain general points are worth attention. As is readily proved from (3.3) and (3.4) by induction over k, $m_{r,s}$ depends only on the terms on the principal diagonal between $m_{u,u}$ and $m_{v,v}$ inclusive, where $u, v = r \pm |r-s|$; indeed it is a linear combination of these terms. It follows from (3.5) that

$$m_{r,s} = 0 \quad \text{for} \quad |r-s| < r. \tag{3.7}$$

Thus for the flow in any layer there are no image sources nearer than the source M itself. An immediate consequence of (3.3) and (3.4) is that if $U_r = U_{r+1}$, then $m_{r,s} = m_{r+1,s}$, and hence as expected the image pattern is the same in the two layers. Near the principal diagonal non-zero images occur only for small values of r, and their strengths depend on the distribution of stream velocity near M itself. It is interesting to compare this with one of Lighthill's main deductions; that when expanded in powers of distance from the source the first-order perturbation is just the source flow itself, and the second-order perturbation depends only on the velocity and shear at $y = 0$.

4. Continuous velocity distribution

For a flow in which the stream velocity U in the x-direction is a continuously varying function of y, equations for the image source distribution representing the effects of a small source M at the origin may be deduced from the analysis of the last section, by taking the layer thickness δ to be small, and replacing U_r and $m_{r,s}$ by $U(y)$ and $m(y,s)$. Thus at the point (x,y,z) the perturbation to the flow is determined by a source distribution along the y-axis, of strength per unit length $m(y,s)$ at $(0,s,0)$.

In equations (3.3) and (3.4) we replace $U_{r+1} - U_r$ by $U'\delta$, where the dash denotes differentiation, and ignore δ^2. Each equation leads to

$$\frac{\partial m}{\partial y}(y,s) + \frac{U'}{U} m(y, 2y-s) = 0. \tag{4.1}$$

To obtain an equation for $m(y,s)$ alone, replace s by $2y-s$ in (4.1), giving

$$\frac{\partial m}{\partial y}(y, 2y-s) + \frac{U'}{U} m(y,s) = 0. \tag{4.2}$$

Here the first term is to be interpreted as the value of $(\partial/\partial y)\, m(y,s)$ at the point $(y, 2y-s)$ in the ys-plane. Differentiation of (4.1) with respect to y and s respectively gives

$$\frac{\partial^2 m}{\partial y^2}(y,s) + \left(\frac{U''}{U} - \frac{U'^2}{U^2}\right) m(y, 2y-s) + \frac{U'}{U}\frac{\partial m}{\partial y}(y, 2y-s) + 2\frac{U'}{U}\frac{\partial m}{\partial s}(y, 2y-s) = 0, \tag{4.3}$$

$$\frac{\partial^2 m}{\partial y \partial s}(y,s) - \frac{U'}{U}\frac{\partial m}{\partial s}(y, 2y-s) = 0, \tag{4.4}$$

and substitution in (4.3) from equations (4.1), (4.2) and (4.4) leads to the required equation for $m(y, s)$

$$\frac{\partial^2 m}{\partial y^2} + 2\frac{\partial^2 m}{\partial y \partial s} + \left(\frac{U'}{U} - \frac{U''}{U'}\right)\frac{\partial m}{\partial y} - \frac{U'^2}{U^2} m = 0. \tag{4.5}$$

This is the fundamental equation for the source function. It may also be deduced directly from (3.6). We are interested in solutions for which $m = 0$ on the line $y = s$, except for a singular source M at $y = 0$, i.e.

$$\lim_{\epsilon \to 0} \int_{-\epsilon}^{\epsilon} m(0, s)\, ds = M, \quad \text{or} \quad m(0, s) = M\delta(s). \tag{4.6}$$

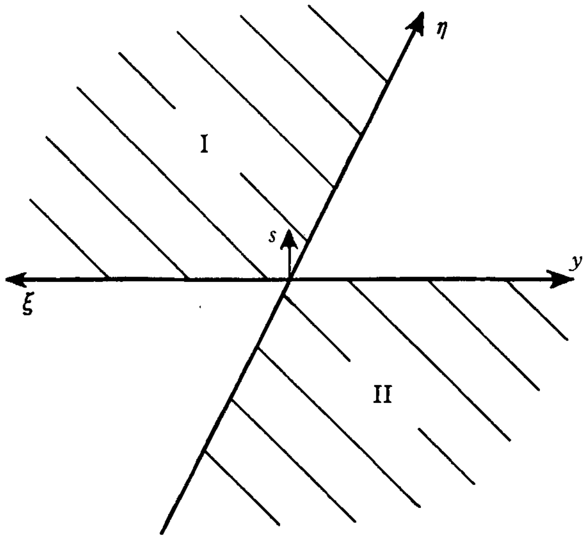

FIGURE 1. The regions I and II in the ys-plane in which the image source distribution $m(y, s)$ is non-zero.

Equation (4.5) is a hyperbolic equation, with characteristics $s - 2y =$ constant and $s =$ constant, and we may conveniently introduce characteristic variables

$$\xi = s - 2y, \quad \eta = s. \tag{4.7}$$

The effects of the source M are therefore confined to the two regions I ($\xi > 0$, $\eta > 0$) and II ($\xi < 0$, $\eta < 0$), as shown in figure 1. This is as was to be anticipated from (3.7). The equation (4.5) may be solved separately for the two regions, though the solutions are connected by (4.1), which relates conditions at a point in I to conditions at a point in II.

As regards the boundary conditions which apply along the boundaries $\xi = 0$ and $\eta = 0$, it is clear from (4.1) with $s = 0$ and (4.6) that there is a singular source of constant strength $M\delta(s)$ along the whole of the y-axis, since m is finite on the line $s - 2y = 0$. Consider next (4.1) with s constant, equal to $2y_1 > 0$, and integrate with respect to y over a short interval including $y = y_1$. Since $m = 0$ for $y > y_1$, the left-hand side gives $-m(y_1, 2y_1)$. The right-hand side gives

$$\lim_{\epsilon \to 0} \frac{U'}{U}(y_1) \int_{-\epsilon}^{\epsilon} m(y_1, 2\theta)\, d\theta = \tfrac{1}{2} M \frac{U'}{U}(y_1).$$

The required boundary condition at $\xi = 0$ in I is therefore

$$m(y, 2y) = \tfrac{1}{2}M \frac{U'}{U}(y) \quad (\eta > 0). \tag{4.8}$$

A similar calculation shows that the corresponding boundary condition at $\xi = 0$ in II is

$$m(y, 2y) = -\tfrac{1}{2}M \frac{U'}{U}(y) \quad (\eta < 0). \tag{4.9}$$

The boundary conditions at $\eta = 0$ are now given by a further application of (4.1). In I, $y < 0$ on $s = 0$ and hence we have

$$\frac{\partial m}{\partial y}(y, 0) = \tfrac{1}{2}M \left\{\frac{U'}{U}(y)\right\}^2 \quad (\xi > 0), \tag{4.10}$$

on making use of (4.9), as is appropriate since the point $(y, 2y)$ is in II. The corresponding condition at $\eta = 0$ in II is

$$\frac{\partial m}{\partial y}(y, 0) = -\tfrac{1}{2}M \left\{\frac{U'}{U}(y)\right\}^2 \quad (\xi < 0). \tag{4.11}$$

These conditions (4.8)–(4.11) are sufficient for the complete solution of (4.5). To be precise, they should be interpreted as giving the limiting values as the boundary is approached from within the region in question, since m is discontinuous or singular on the boundary. It is easy to write down integrated forms of (4.10) and (4.11) which give $m(y, 0)$ directly, since $m(0, 0)$ is known from equations (4.8) and (4.9), but the forms given are usually the most convenient.

Before proceeding further we must refer to an important point in regard to the velocity field which corresponds to the source distribution. For uniform flow with velocity discontinuities, as considered in §3, the perturbation velocity presents no difficulties, being merely that due to the set of image sources appropriate for the particular layer. But for a continuously varying stream the velocity field due to the source distribution $m(y, s)$, $-\infty < s < \infty$, is not the whole perturbation velocity. The stream surface at (x, y, z) has been displaced a distance d, say, in the y-direction from its undisturbed position, and in consequence the stream velocity at (x, y, z) is that at $(x, y-d, z)$ in the undisturbed flow. Thus there is an additional perturbation velocity in the x-direction of amount $u_c = -dU'$, since d is small for a weak source. Now we may write

$$d = \int_{-\infty}^{x} \frac{v}{U}\, dx, \tag{4.12}$$

since the perturbation is small and hence

$$u_c = -\frac{U'}{U}\int_{-\infty}^{x} v\, dx, \quad \frac{\partial u_c}{\partial x} = -\frac{U'}{U} v. \tag{4.13}$$

The velocity given by (4.13) makes a contribution to the continuity equation

$$\frac{\partial u}{\partial x} + \frac{\partial v}{\partial y} + \frac{\partial w}{\partial z} = 0, \tag{4.14}$$

which must be satisfied everywhere except at the origin. This at first looks unpromising, but it is soon apparent that the velocity field due to the image sources themselves does *not* satisfy (4.14). The flow due to a fixed set of sources would of course do so, and the displacements which determine $\partial u/\partial x$ and $\partial w/\partial z$ do not involve any change in the source distribution. But a displacement in the y-direction does cause the image system $m(y,s)$ to alter, and so $\partial v/\partial y$ contains an extra, unbalanced, term. We can show that this term is precisely that needed to cancel the contribution from (4.13).

Due to the image sources, the velocity in the y-direction at (x,y,z) is

$$v = \int_{-\infty}^{\infty} m(y,s)\frac{y-s}{4\pi\rho^3}ds, \tag{4.15}$$

where ρ is the distance between the points $(0,s,0)$ and (x,y,z). The unbalanced term in $\partial v/\partial y$ is that due to the variation of $m(y,s)$, namely

$$\begin{aligned}\int_{-\infty}^{\infty}\frac{\partial m}{\partial y}(y,s)\frac{y-s}{4\pi\rho^3}ds &= -\frac{U'}{U}\int_{-\infty}^{\infty} m(y,2y-s)\frac{y-s}{4\pi\rho^3}ds \\ &= \frac{U'}{U}\int_{-\infty}^{\infty} m(y,s_1)\frac{y-s_1}{4\pi\rho_1{}^3}ds_1 \\ &= \frac{U'}{U}v \end{aligned} \tag{4.16}$$

by (4.1), where $s_1 = 2y-s$ and ρ_1 is the distance between $(0,s_1,0)$ and (x,y,z). This is the required result, and confirms the consistency of our equations.

It may be remarked that all our analysis may be applied immediately to the simpler problem of a purely two-dimensional disturbed flow. If the point source M at the origin is replaced by a line source of strength M per unit length along the z-axis, the strength of the image source distribution $m(y,s)$ has precisely the same form as for the three-dimensional flow with the same stream velocity $U(y)$, since all the conditions used in deriving the equations for $m(y,s)$ are unchanged. The velocity field is of course different, since the velocity due to each source element falls off like the inverse first power instead of the inverse square of the distance from the source.

A further point of interest concerns the nature of the fluid emitted from the source. In the discrete-layer model of the shear flow described in § 3, the fluid from the source emerges into a layer of uniform stream velocity, and naturally is itself irrotational. The source is not affected by the limiting process in which the layers become increasingly narrow and numerous, and so in the continuous-velocity flow the source fluid is still irrotational. In two-dimensional perturbed flow with constant verticity ω_0, this is not always assumed to be the case. It is then often convenient to write down a solution for the velocity field which has vorticity ω_0 everywhere, including the regions occupied by fluid which has emerged from a source. Such solutions are therefore not immediately comparable with the results of the present theory.

In this paper we shall make no further reference to the case of purely two-dimensional disturbed flow. The calculation of the corresponding velocity field presents no new difficulties.

5. Special solutions

Further progress can be made only with more definite assumptions about the form of the stream velocity distribution $U(y)$. We shall here concentrate chiefly on simple shear flow, for which $U = a(y+y_0)$, but first we shall briefly investigate what other velocity distributions are tractable.

First, we may note that (4.5) is unchanged if $U(y)$ is replaced by $U^*(y) = 1/U(y)$, and hence the same general solution $m(y,s)$ is applicable. The boundary conditions (4.8) and (4.9) change sign, but not conditions (4.10) and (4.11), and so the particular solution required will be different.

The form of (4.5) is simplified in three cases. These are when the coefficient of m is zero, when the coefficient of $\partial m/\partial y$ is zero, and when the equation can be immediately integrated with respect to y. We shall examine each of these in turn, and shall find that the special cases considered by Lighthill (1957*c*) will all be included.

The term $(U'^2/U^2)m$ in (4.5) is small compared with the other terms when the relative velocity change through the sheer layer is small. If this term is neglected (4.5) becomes

$$\left(\frac{\partial}{\partial y}+2\frac{\partial}{\partial s}\right)\log\left(\frac{U}{U'}\frac{\partial m}{\partial y}\right) = 2\frac{\partial}{\partial \eta}\log\left(\frac{U}{U'}\frac{\partial m}{\partial y}\right) = 0, \tag{5.1}$$

on introducing the characteristic variables (4.7). Hence

$$\frac{\partial m}{\partial y} = \frac{U'}{U}F(\xi) = \frac{U'}{U}F(s-2y), \tag{5.2}$$

where $F(\xi)$ is an arbitrary function. In region I, (4.10) shows that

$$F(-2y) = \tfrac{1}{2}M\frac{U'}{U}(y).$$

Equation (5.2) can now be integrated with respect to y to give

$$m = G(s)+\tfrac{1}{2}M\int_{\frac{1}{2}s}^{y}\frac{U'}{U}(t)\frac{U'}{U}(t-\tfrac{1}{2}s)\,dt. \tag{5.3}$$

From (4.8) the arbitrary function $G(s)$ satisfies

$$G(2y) = \tfrac{1}{2}M\frac{U'}{U}(y).$$

The solution for region I is therefore

$$m = \tfrac{1}{2}M\frac{U'}{U}(\tfrac{1}{2}s)-\tfrac{1}{2}M\int_{y}^{\frac{1}{2}s}\frac{U'}{U}(t)\frac{U'}{U}(t-\tfrac{1}{2}s)\,dt. \tag{5.4}$$

In region II, the boundary conditions (4.9) and (4.11) show that the required expression for m is that of (5.4), with the sign changed.

The solution may be improved by using (5.4) to approximate to the neglected term in (4.5). The integration to find the extra contribution to m is quite straightforward, and the boundary conditions have already been satisfied exactly. The result for region I is

$$\frac{2m}{M} = \frac{U'}{U}(\tfrac{1}{2}s) - \int_y^{\frac{1}{2}s} \frac{U'}{U}(t)\frac{U'}{U}(t-\tfrac{1}{2}s)\,dt - \int_y^{\frac{1}{2}s}\frac{U'}{U}(u)\,du\int_0^{\frac{1}{2}s}\frac{U'}{U}(t+u-\tfrac{1}{2}s)\frac{U'}{U}(t)\,dt$$
$$+\int_y^{\frac{1}{2}s}\frac{U'}{U}(v)\,dv\int_0^{\frac{1}{2}s}\frac{U'}{U}(u+v-\tfrac{1}{2}s)\,du\int_{u+v-\frac{1}{2}s}^{u}\frac{U'}{U}(t)\frac{U'}{U}(t-u)\,dt. \quad (5.5)$$

In region II the sign is changed. The process of successive approximation may be repeated as often as required.

Lighthill (1957*c*) considered a shear layer with what he called 'small velocity spread', and obtained the equivalent of the first term of (5.5) in the form $m = \frac{1}{2}MU'(\frac{1}{2}s)/U(0)$. A direct application of the formulae of §2 leads to this result, and indeed also to the fuller result (5.5), and is of interest as indicating the physical significance of the successive terms in the solution.

Suppose that the shear layer is replaced by N layers of uniform flow, each of thickness δ, separated by vortex sheets each of strength $O(\epsilon)\,U$, where ϵ is small. From (2.3) the transmitted source at one of the vortex sheets is $M\{1+O(\epsilon^2)\}$, and hence from the source at the origin to the observation point (x, y, z) the transmitted source is changed to $M\{1+O(N\epsilon^2)\}$. The shear layer may be considered to be the limiting case where $\delta \to 0$, $N \to \infty$ and $\epsilon \to 0$, the total velocity change of magnitude $O(N\epsilon)\,U$ remaining fixed. The source M is therefore transmitted unaltered. From (2.3) the image source m_i due to a velocity discontinuity $k\epsilon U$ passing through $(0, l, 0)$, where $l > y > 0$, is $m_i = M\{k\epsilon + O(\epsilon^2)\}$. These images sources m_i are spaced at intervals 2δ along the y-axis, and so the source density at $(0, 2l, 0)$ is approximately $Mk\epsilon/2\delta$. Now as $\delta \to 0$, $k\epsilon/\delta \to (U'/U)\,(l)$, and hence the sources m_i combine to form the distribution $m(y,s) = \frac{1}{2}M(U'/U)\,(\frac{1}{2}s)$, $s > 2y$, exactly as given by the first term of (5.5). For $0 < l < y$ there is no image source m_i and for $l < 0$ there is agreement in region II, as is seen most easily by reversing the direction of the y-axis.

The primary images m_i which are appropriate at $(0, t, 0)$ will have secondary images in the vortex sheet passing through this point, provided that they are on the same side of the sheet as the observation point (x, y, z). The total strength of the primary images is $O(N\epsilon)\,M$, and hence the set of secondary images in the N discontinuities has total strength $O(N^2\epsilon^2)\,M$. If the relative velocity spread across the layer is small, $N\epsilon$ is small, and only the primary images are of importance. This is in accord with Lighthill's result. The source density due to the secondary images may be shown to agree with the second term of (5.5), by an extension of the analysis given above. That the velocity discontinuities are appropriately situated is seen by constructing diagrams as shown in figure 2, considering the image sources to be due to reflexions in the vortex sheets. Further diagrams and calculations check that the later terms of (5.5) correctly represent the effects of third- and fourth-order images. The physical interpretation of the terms in the series solution (5.5) is thus well established.

If the velocity is uniform outside the range $-a < y < b$, the primary images are clearly confined to the interval $-2a < s < 2b$, and the secondary images are confined to $-2(a+b) < s < 2(a+b)$, for otherwise the corresponding integrand in (5.5) is nowhere non-zero. In each case there are no sources in the range $|s-y| < y$. Similarly, the third-order images are confined to

$$-4a-2b < s < 2a+4b,$$

and the fourth order to $-4(a+b) < s < 4(a+b)$. These results are also readily deduced from diagrams like those of figure 2.

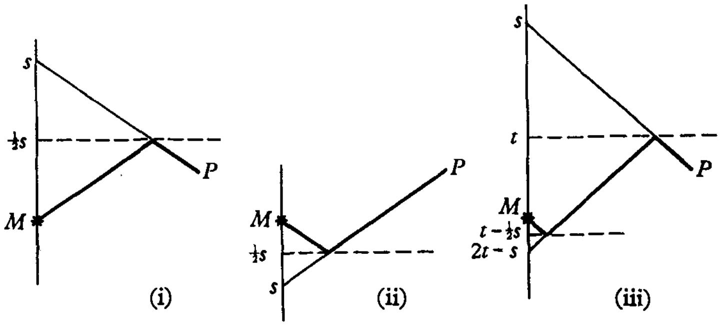

FIGURE 2. Illustrations of the location of primary and secondary images of the point source M at the origin, as observed at $P(x, y, z)$: (i) a primary image with $s > 2y > 0$; (ii) a primary image with $s < 0$; (iii) a secondary image. ———, paths of reflexion; -----, vortex sheets at which reflexion takes place.

In the second case we are to examine, the coefficient of $\partial m/\partial y$ in (4.5) is zero. This occurs when $U'/U = U''/U'$, i.e. when $U = a e^{\lambda y}$, where a and λ are constants. This case proved easy to solve by Lighthill's method. Equation (4.5) reduces to

$$\frac{\partial^2 m}{\partial y^2} + 2\frac{\partial^2 m}{\partial y\,\partial s} - \lambda^2 m = 0, \tag{5.6}$$

which in terms of the variables (ξ, η) of (4.7) becomes

$$4\frac{\partial^2 m}{\partial \xi\,\partial \eta} + \lambda^2 m = 0. \tag{5.7}$$

The boundary conditions (4.8) and (4.10) in region I give

$$m(0,\eta) = \tfrac{1}{2}M\lambda, \quad m(\xi, 0) = \tfrac{1}{2}M\lambda(1-\tfrac{1}{2}\lambda\xi). \tag{5.8}$$

The required solution of (5.7) is readily deduced from the form of solution given by Courant & Hilbert (1937, ch. v, §4.3). It is

$$\begin{aligned}\frac{2m}{M\lambda} &= J_0(\lambda\xi^{\frac{1}{2}}\eta^{\frac{1}{2}}) - \xi^{\frac{1}{2}}\eta^{-\frac{1}{2}}J_1(\lambda\xi^{\frac{1}{2}}\eta^{\frac{1}{2}})\\ &= J_0\{\lambda(s-2y)^{\frac{1}{2}}y^{\frac{1}{2}}\} - (s-2y)^{\frac{1}{2}}s^{-\frac{1}{2}}J_1\{\lambda(s-2y)^{\frac{1}{2}}s^{\frac{1}{2}}\}.\end{aligned} \tag{5.9}$$

For region II the boundary conditions (5.8) have their signs changed, and remembering that ξ and η are negative the solution is seen to be

$$\begin{aligned}\frac{2m}{M\lambda} &= -J_0\{\lambda(-\xi)^{\frac{1}{2}}(-\eta)^{\frac{1}{2}}\} - (-\xi)^{\frac{1}{2}}(-\eta)^{-\frac{1}{2}}J_1\{\lambda(-\xi)^{\frac{1}{2}}(-\eta)^{\frac{1}{2}}\}\\ &= -J_0\{\lambda(2y-s)^{\frac{1}{2}}(-s)^{\frac{1}{2}}\} - (2y-s)^{\frac{1}{2}}(-s)^{-\frac{1}{2}}J_1\{\lambda(2y-s)^{\frac{1}{2}}(-s)^{\frac{1}{2}}\}.\end{aligned} \tag{5.10}$$

The velocity distribution corresponding to this source distribution may be worked out by precisely the same techniques as those employed in §6, and the author has confirmed that the formulae given by Lighthill (1957*c*) are obtained, on making use of standard integral relations between Bessel functions.

The third special case is that in which (4.5) is immediately integrable with respect to y. For this to be possible

$$\frac{d}{dy}\left(\frac{U'}{U}-\frac{U''}{U'}\right)=-\frac{U'^2}{U^2},$$

and hence

$$\frac{U''}{U}+\frac{U''^2}{U'^2}-\frac{U'''}{U'}=0. \tag{5.11}$$

This is satisfied if $U''=0$, which is simple shear flow $U=a(y+y_0)$. If $U''\neq 0$, (5.11) multiplied by U'/U'' may be integrated to give

$$\log(UU'/U'')=\text{constant}. \tag{5.12}$$

A further integration gives

$$U'=c+dU^2, \tag{5.13}$$

where c and d are constants. The integral of this equation takes one of the forms $U=a(y+y_0)$, $a/(y+y_0)$, $a\tan b(y+y_0)$, $a\tanh b(y+y_0)$, $a\coth b(y+y_0)$. For all these velocity distributions the integration of (4.5) proceeds in a manner closely analagous to that for simple shear flow, to be treated in §6. It may be verified that for the stream $U=a\tanh b(y+y_0)$ the solution in region I is

$$m=Mb\frac{\sinh b(2y-s+y_0)}{\sinh by_0\sinh 2b(y+y_0)}, \tag{5.14}$$

in region II the sign being reversed. By suitable modifications of the constants a and b the solutions for the other streams listed above may now be written down.

It may be argued that some of these velocity distributions are unrealistic, in view of the occurrence of points at which the velocity changes sign or becomes infinite. However, it is possible to consider that a form of velocity distribution holds only over a limited range of y, as will be seen in §7.

6. Simple shear flow

For simple shear flow, $U=a(y+y_0)$ and equation (4.5) becomes

$$\frac{\partial^2 m}{\partial y^2}+2\frac{\partial^2 m}{\partial y\,\partial s}+\frac{1}{y+y_0}\frac{\partial m}{\partial y}-\frac{1}{(y+y_0)^2}m=0. \tag{6.1}$$

This may be integrated immediately with respect to y to give

$$\frac{\partial m}{\partial y}+2\frac{\partial m}{\partial s}+\frac{m}{y+y_0}=G(s). \tag{6.2}$$

In terms of the variable (ξ,η) of (4.7) this may be written in the form

$$2\frac{\partial}{\partial\eta}\{m(y+y_0)\}=(y+y_0)\,G(s). \tag{6.3}$$

The boundary conditions (4.8) and (4.10) in region I are

$$m(y, 2y) = m(0, \eta) = \frac{\frac{1}{2}M}{y+y_0}, \tag{6.4}$$

$$\frac{\partial m}{\partial y}(y, 0) = \frac{\partial m}{\partial y}(\xi, 0) = \frac{\frac{1}{2}M}{(y+y_0)^2}, \tag{6.5}$$

and by applying (6.4) to equation (6.3) on the line $\xi = 0$ we see that $G(s) = 0$. We can therefore integrate (6.3) with respect to η to obtain

$$m(y+y_0) = F(\xi) = F(s-2y). \tag{6.6}$$

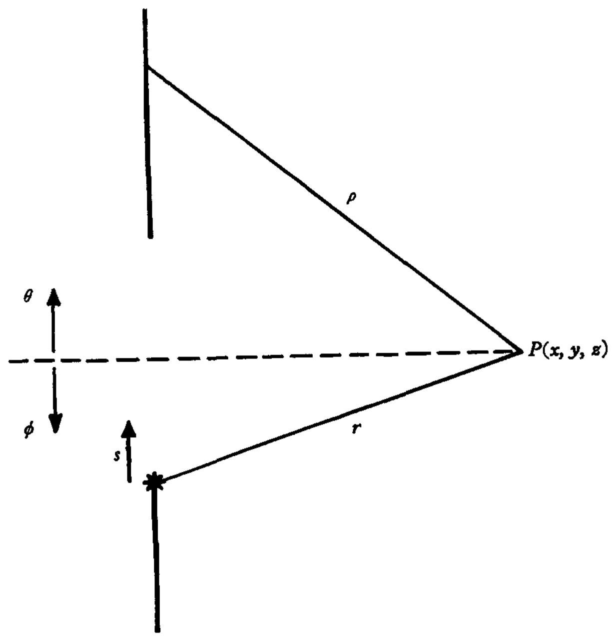

FIGURE 3. Location of the image sources $m(y, s)$, and notation used in calculating the velocity components.

On the line $s = 0$, (6.5) gives

$$m(y, 0) = \frac{M}{y_0} - \frac{M}{2(y+y_0)} = \frac{M(2y+y_0)}{2y_0(y+y_0)} \tag{6.7}$$

since, from (6.4), $m(0, 0) = \frac{1}{2}M/y_0$. Hence from (6.6)

$$m = \frac{M(2y-s+y_0)}{2y_0(y+y_0)}. \tag{6.8}$$

In region II the sign is changed in equations (6.4) and (6.5), and hence

$$m = -\frac{M(2y-s+y_0)}{2y_0(y+y_0)}. \tag{6.9}$$

Note that (6.8) is equal to the limiting value of (5.14) as $b \to 0$.

Consider now the velocity perturbation at the point $P(x, y, z)$ due to a source M at the origin. The image source strength $m(y, s)$ at $(0, s, 0)$ is given by (6.8) and (6.9). For $y > 0$ the situation is as shown in figure 3. It is convenient to introduce co-ordinates θ and ϕ as shown, to describe the positions of the image sources in regions I and II respectively. Thus

$$\theta = s-y, \quad \phi = y-s. \tag{6.10}$$

In terms of these, equations (6.8) and (6.9) become

$$\left.\begin{aligned} \frac{2y_0 m}{M} &= 1-\frac{\theta}{y+y_0} \quad (\theta > y), \\ \frac{2y_0 m}{M} &= -1-\frac{\phi}{y+y_0} \quad (\phi > y). \end{aligned}\right\} \tag{6.11}$$

Pairs of points at which θ and ϕ are equal are symmetrically situated with respect to P, and hence the sources corresponding to the terms 1 and -1 in (6.11) have no net effect on u and w, and equal effects on v. Similarly, the other terms of (6.11) have no net effect on v, but equal effects on u and w.

The contribution to v from the source distribution (6.11) is

$$v_s = -\frac{M}{y_0}\int_y^\infty \frac{\theta}{4\pi\rho^3}d\theta = \frac{M}{4\pi y_0}\left[\frac{1}{\rho}\right]_y^\infty = -\frac{M}{4\pi y_0 r}, \tag{6.12}$$

where $\rho = (x^2+\theta^2+z^2)^{\frac{1}{2}}$ is the distance of the image source from P, and $r = (x^2+y^2+z^2)^{\frac{1}{2}}$. There is also the velocity due to the source M itself, giving $v_M = My/(4\pi r^3)$. The total y-component of the perturbation velocity is therefore

$$v = v_M + v_s = \frac{M}{4\pi}\left(\frac{y}{r^3}-\frac{1}{y_0 r}\right). \tag{6.13}$$

Similarly the x-component due to the source distribution is

$$u_s = -\frac{M}{y_0(y+y_0)}\int_y^\infty \theta\frac{x}{4\pi\rho^3}d\theta = -\frac{Mx}{4\pi y_0(y+y_0)r}, \tag{6.14}$$

the integral being of the same form as that occurring above, and $u_M = Mx/(4\pi r^3)$. We have also to include the convective component u_c as given by (4.13). This equation shows that

$$\frac{\partial u_c}{\partial x} = -\frac{v}{y+y_0} = -\frac{M}{4\pi(y+y_0)}\left(\frac{y}{r^3}-\frac{1}{y_0 r}\right),$$

and hence
$$u_c = -\frac{M}{4\pi(y+y_0)}\left\{\frac{xy}{(y^2+z^2)r}-\frac{1}{y_0}\log(r+x)+f(y,z)\right\}. \tag{6.15}$$

The arbitrary function $f(y,z)$ presents difficulties, since $\log(r+x)$ becomes logarithmically infinite at $x=\pm\infty$. If we require u_c to be zero at $x=0$, then we should write $f(y,z) = (1/2y_0)\log(y^2+z^2)$, and

$$\begin{aligned} u &= u_M+u_s+u_c \\ &= \frac{M}{4\pi}\left\{\frac{x}{r^3}-\frac{x}{y_0(y+y_0)r}-\frac{xy}{(y+y_0)(y^2+z^2)r}+\frac{1}{2y_0(y+y_0)}\log\frac{r+x}{r-x}\right\}. \end{aligned} \tag{6.16}$$

Finally, w has precisely the same form as u, except that no convective term is present, and so

$$w = \frac{M}{4\pi}\left\{\frac{z}{r^3}-\frac{z}{y_0(y+y_0)r}\right\}. \tag{6.17}$$

These velocity components are in accord with those given by Lighthill (1957*c*). Although they have been derived only for $y > 0$, a consideration of the effect of reversing the direction of the y-axis shows that the formulae all hold unchanged for $y < 0$.

Lighthill described the infinity in u as 'an extremely discouraging feature'. The author's view is rather more optimistic. The occurrence of the infinity emphasizes the artificial nature of the assumption that the uniform shear extends indefinitely in all directions. In practice there are always constraining boundaries to limit the drift of streamlines. For that is what causes the trouble in (6.16). The displacement d in the y-direction of streamlines between $x = 0$ and $x = \pm\infty$, as given by (4.12), is logarithmically infinite. This is nothing peculiar to shear layers; the same is true for the flow with circulation past a cylinder. But it does indicate that in any attempt to make measurements of the Pitot-tube displacement effect the nature of the boundaries to the shear flow, however distant, has a vital influence. In some cases (6.16) could probably be used quite effectively by taking given undisturbed conditions to be attained not at $x = -\infty$ but at some plausible position $x = -x_0$. If the shear flow terminates at planes $y =$ constant, the modified image source distribution may be determined as shown below.

A more serious objection to placing reliance on the solution obtained in this section is that the stream velocity falls to zero at $y = -y_0$. This invalidates the basic assumption on which the whole method of analysis is based, starting from equations (2.1) and (2.2). Indeed we have no real reason to suppose that our solution is reliable *anywhere*, since the true source distribution $m(y, s)$, if one exists, might well obey conditions at $y = -y_0$ which are quite different from those obeyed by the solutions (6.8) and (6.9).

7. Bounded shear flows

In flows occurring in practice it will happen only rarely that the velocity distribution $U(y)$ in the undisturbed shear layer can be considered to have the same simple analytic form for all y. Either the flow will be terminated by solid or free boundaries, or the velocity will become uniform outside a certain range of values of y. The analysis given in this paper can be extended to determine the image source distribution for streams in which the form $U(y)$ changes abruptly at some value $y = -y_1$, the expressions for $U(y)$ in both the regions $y > -y_1$ and $y < -y_1$ being ones for which solutions have been found. A discontinuity in $U(y)$ at $y = -y_1$ is permissible.

For simplicity we shall here examine in detail only the stream consisting of simple shear flow $U = a(y+y_0)$ in the region $y > -y_1$ and uniform flow $U = U_0$ in $y < -y_1$. There is then a velocity discontinuity $U_1 - U_0$ at $y = -y_1$, where $U_1 = a(y_0 - y_1)$.

The regions of the ys-plane in which $m(y, s)$ has to be determined are shown in figure 4. In A and A^* the source distributions are given by equations (6.8) and (6.9), since the hyperbolic nature of (6.1) shows that the effects of the change at $y = -y_1$ cannot extend beyond the lines $2y - s + 2y_1 = 0$ and $s + 2y_1 = 0$. From (4.1), m is independent of y for $y < -y_1$, since U is constant, and in particular $m = 0$ in C^*. The relations which hold across the line $y = -y_1$ are now given by equations (3.3) and (3.4) as

$$(U_1^2+U_0^2)\,m(-y_1,s)_C = 2U_1U_0m(-y_1,s)_B, \tag{7.1}$$

$$m(-y_1, 2y-s)_{B^*} = \alpha m(-y_1,s)_B, \tag{7.2}$$

where $\alpha = (U_0^2-U_1^2)/(U_0^2+U_1^2)$. We also see from (3.4) or (2.3) that there is a concentrated source $\alpha M\delta(s+2y_1)$ for $y > -y_1$ and hence, as for (4.8) and (6.4), m has a discontinuity $\frac{1}{2}\alpha M(y+y_0)$ on passing from A to B across the line $2y-s+2y_1 = 0$.

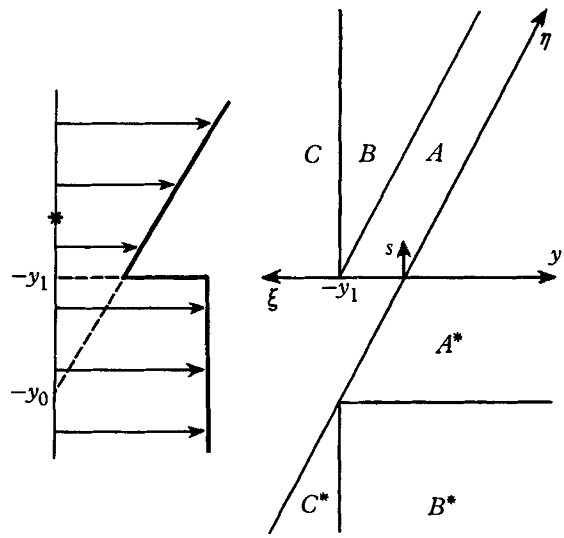

FIGURE 4. Undisturbed velocity distribution in a shear layer bounded at $y = -y_1$, and the regions of the ys-plane in which $m(y, s)$ has to be determined.

We require a more general solution of (6.3) than the form (6.8). If in (6.3) we for convenience replace the arbitrary function $G(s)$ by $4G''(s)$ the equation becomes

$$\frac{\partial}{\partial\eta}\{m(y+y_0)\} = (\eta-\xi+2y_0)\,G''(\eta), \tag{7.3}$$

which gives on integration

$$m(y+y_0) = (\eta-\xi+2y_0)\,G'(\eta)-G(\eta)+F(\xi). \tag{7.4}$$

Reverting to the variables (y, s) we obtain as the general solution of (6.3)

$$m = \frac{F(s-2y)}{y+y_0}+\frac{2(y+y_0)\,G'(s)-G(s)}{y+y_0}. \tag{7.5}$$

The solution (6.8) is given by $F = \frac{1}{2}M(2y-s+y_0)/y_0$, $G = 0$ and also by $F = 0$, $G = \frac{1}{2}M(s+y_0)/y_0$. The first of these forms of solution may be said to be propagated in the η-direction (along lines ξ = constant) and the second in the ξ-direction (along lines η = constant). It is a useful fact that either form is appropriate for unlimited simple shear flow.

In the present problem the solution in region A may be taken to be in the η-direction, and consequently the same must be true in B, so that there

$$m = \frac{F(s-2y)}{y+y_0}. \tag{7.6}$$

The boundary condition (7.2) combined with (4.1) gives

$$\frac{\partial m}{\partial y}(-y_1, s) = -\frac{\alpha}{y_0-y_1} m(-y_1, s), \tag{7.7}$$

and on substituting the form (7.6) we obtain at once

$$F = F_0 \exp\left[\frac{(1-\alpha)(2y-s)}{2(y_0-y_1)}\right] \tag{7.8}$$

provided that $\alpha \neq 1$. The discontinuity of m on $2y-s+2y_1 = 0$, as found above, enables the constant F_0 to be determined and gives us the final result for region B

$$m = \frac{M\{(\alpha+1)y_0-2y_1\}}{2y_0(y+y_0)} \exp\left[\frac{(1-\alpha)(2y-s+2y_1)}{2(y_0-y_1)}\right]. \tag{7.9}$$

Equation (4.2) now shows that in B^*

$$m = \frac{M\{(\alpha+1)y_0-2y_1\}\{(\alpha-1)y+\alpha y_0-y_1\}}{2y_0(y_0-y_1)(y+y_0)} \exp\left[\frac{(1-\alpha)(s+2y_1)}{2(y_0-y_1)}\right]. \tag{7.10}$$

When $\alpha = 1$, (7.8) is replaced by $F = F_0$ and we obtain

$$m = \frac{M(y_0-y_1)}{y_0(y+y_0)} \tag{7.11}$$

in both B and B^*, as would be given by putting $\alpha = 1$ in equations (7.9) and (7.10). In region C equations (7.1) and (7.9), and the condition that m is independent of y, show that

$$m = \frac{2U_1U_0}{U_1^2+U_0^2} \frac{M\{(\alpha+1)y_0-2y_1\}}{2y_0(y_0-y_1)} \exp\left[\frac{(\alpha-1)s}{2(y_0-y_1)}\right], \tag{7.12}$$

and from (2.3) there is in addition a concentrated source

$$\frac{2U_1U_0}{U_1^2+U_0^2} M\delta(s)$$

for $y < -y_1$.

When $\alpha = 1$, $U_0 = \infty$. Such a stream could not be deflected by any finite pressure force, so the solution applies for a solid wall at $y = -y_1$. Other cases of practical interest are $\alpha = 0$, corresponding to no discontinuity of stream velocity at $y = -y_1$ but merely a change from uniform shear to constant velocity, and $\alpha = -1$, for which the fluid in the region $y < -y_1$ is at rest. Since $-1 \leqslant \alpha \leqslant 1$ the image source strength in both B and B^* decreases exponentially with distance from the origin (except when $\alpha = 1$), provided that $y_0 > y_1$, i.e. provided that there is no plane of zero stream velocity in the physical flow. If $y_0 < y_1$ the sources increase exponentially with distance, which again emphasizes the unreality of solutions for streams in which the velocity passes through zero.

The calculation of the velocity fields corresponding to these source distributions is a straightforward extension of that for an unbounded simple shear flow, although unless $\alpha = 1$ the results cannot be expressed in terms of elementary functions. For $\alpha = 1$, with a solid wall at $y = -y_1$, the image source distribution in terms of the co-ordinates θ and ϕ of (6.10) is given by

$$\frac{2y_0 m}{M} = \left\{\begin{array}{ll} 2\dfrac{y_0 - y_1}{y - y_0} & (\theta > y + 2y_1), \\ 1 - \dfrac{\theta}{y + y_0} & (y + 2y_1 > \theta > y), \\ -1 - \dfrac{\phi}{y + y_0} & (y + 2y_1 > \phi > y), \\ 2\dfrac{y_0 - y_1}{y + y_0} & (\phi > y + 2y_1). \end{array}\right\} \tag{7.13}$$

The integrations to find the velocity components are so similar to those of §6 that it will be sufficient to quote the results.

$$u = \frac{M}{4\pi(y+y_0)}\left\{x(y+y_0)\left(\frac{1}{r^3}+\frac{1}{r_1{}^3}\right)+\frac{x}{y_0}\left(\frac{1}{r_1}-\frac{1}{r}\right)+\frac{2(y_0-y_1)x}{u_0 r_1(r_1+y+2y_1)}\right.$$
$$\left.-\left[\frac{y}{r(r-x)}+\frac{y+2y_1}{r_1(r_1-x)}+\frac{1}{y_0}\log\frac{r-x}{r_1-x}\right]\right\}, \tag{7.14}$$

$$v = \frac{M}{4\pi}\left\{\frac{y}{r^3}+\frac{y+2y_1}{r_1{}^3}+\frac{1}{y_0}\left(\frac{1}{r_1}-\frac{1}{r}\right)\right\}, \tag{7.15}$$

$$w = \frac{M}{4\pi(y+y_0)}\left\{z(y+y_0)\left(\frac{1}{r^3}+\frac{1}{r_1{}^3}\right)+\frac{z}{y_0}\left(\frac{1}{r_1}-\frac{1}{r}\right)+\frac{2(y_0-y_1)z}{y_0 r_1(r_1+y+2y_1)}\right\}, \tag{7.16}$$

where $r_1 = \{x^2+(y+2y_1)^2+z^2\}^{\frac{1}{2}}$ is the distance from P to the concentrated image source M at $s = -2y_1$. The term in u enclosed in square brackets represents the convective component u_c, and the arbitrary function of y and z appearing in it has been chosen so that $u_c \to 0$ as $x \to -\infty$. The difficulty in this respect for an unlimited shear layer no longer arises, for any value of α.

The value (u_w, v_w, w_w) of the perturbation velocity at the wall is found by putting $y = -y_1$, $r_1 = r = (x^2+y_1{}^2+z^2)^{\frac{1}{2}}$ in equations (7.14), (7.15) and (7.16). The result is

$$v_w = 0, \quad \frac{u_w}{x} = \frac{w_w}{z} = \frac{M}{2\pi}\left\{\frac{1}{r^3}+\frac{1}{y_0 r(r+y_1)}\right\}. \tag{7.17}$$

8. Shear flow in a channel

When the shear flow is bounded both above and below, at $y = y_2$ and at $y = -y_1$, an infinite series of regions in the ys-plane has to be considered, corresponding to multiple reflexions in the boundaries. The regions are periodic in the s-direction with period $2(y_1+y_2)$, as illustrated in figure 5. For simple shear flow $U = a(y+y_0)$ with solid boundaries at $y = y_2$ and $y = -y_1$ the image source distributions in A and B are given by equations (6.8) and (7.11). The source distribution in C may also be deduced from (7.11) by reversing the direction of the y-axis and replacing y_0 by $-y_0$ and y_1 by y_2. We find that in C

$$m = -\frac{M(y_0+y_2)}{y_0(y+y_0)}, \tag{8.1}$$

and we also see that there is concentrated source $M\delta(s-2y_2)$ for $y < y_2$. Since the solution in the whole region made up of A, B, C and D must be expressible in the form (7.5), and so is the sum of solutions propagated in the ξ- and η-directions,

$$m_A + m_D = m_B + m_C, \tag{8.2}$$

which shows that in D

$$m = -\frac{M(2y-s+2y_1+2y_2+y_0)}{2y_0(y+y_0)}. \tag{8.3}$$

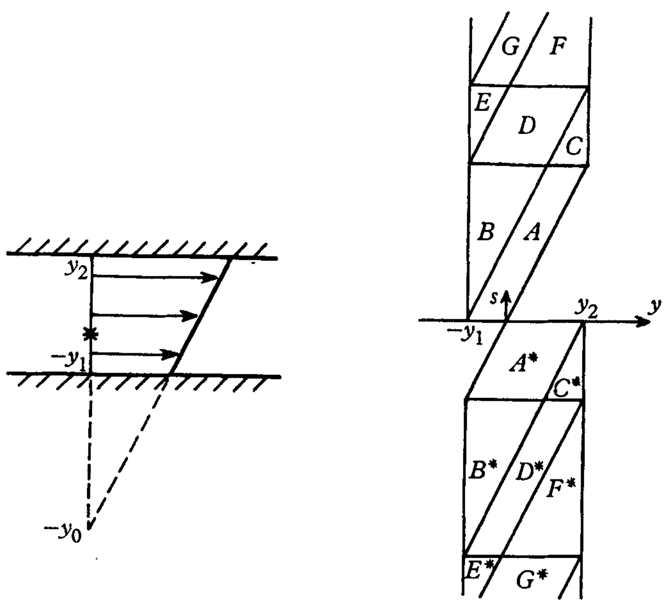

FIGURE 5. Undisturbed velocity distribution in a shear layer bounded at $y = -y_1$ and at $y = y_2$, and the regions of the ys-plane in which $m(y, s)$ has to be determined.

The regions D and A^* are seen from figure 5 to be geometrically identical, and furthermore a comparison of equations (6.9) and (8.3) shows that the source strengths at corresponding points are equal, since the point (y, s) in D corresponds to the point $(y, s-2y_1-2y_2)$ in A^*. Since conditions in D completely determine the source distribution in more distant regions it is clear that m is periodic in the s-direction, with period $2(y_1+y_2)$; in particular $m = 0$ in regions E, F, E^* and F^*. This is not true if the boundaries at $y = -y_1$ and $y = y_2$ are not solid, for then the source strengths in B and C vary exponentially with s, as shown by equations (7.9) and (7.10).

The evaluation of the velocity components corresponding to the periodic source distribution is aided by a formula derived by Olver (1949) and Reuter

(1949) which expresses the potential of an infinite row of point sources as a series of Bessel functions. The formula states that if $h(n) = \{x^2+(y-n)^2\}^{-\frac{1}{2}}$, then

$$\sum_{-\infty}^{\infty} h(n) = \sum_{t=1}^{\infty} K_0(2\pi t x)\cos(2\pi t y) + \text{constant}. \tag{8.4}$$

Since $K_0(z) \sim (\pi/2z)\,e^{-z}$ as $z\to\infty$, the series converges rapidly unless x is very small. This formula and its derivatives with respect to x and y lead to the following results:

$$v = \frac{M}{\pi y_0(y_1+y_2)}\sum_{t=1}^{\infty} K_0\left(\frac{\pi t(x^2+z^2)^{\frac{1}{2}}}{y_1+y_2}\right)\left(\frac{\pi t y_0}{y_1+y_2}\cos\frac{\pi t y_1}{y_1+y_2} - \sin\frac{\pi t y_1}{y_1+y_2}\right)\sin\frac{\pi t(y+y_1)}{y_1+y_2}, \tag{8.5}$$

$$\frac{u-u_c}{x} = \frac{w}{z} = \frac{M}{\pi y_0(y_1+y_2)(y+y_0)(x^2+z^2)^{\frac{1}{2}}}\left\{\frac{(y_0-y_1)(y_0+y_2)}{2(x^2+z^2)^{\frac{1}{2}}} + \sum_{t=1}^{\infty} K_1\left(\frac{\pi t(x^2+z^2)^{\frac{1}{2}}}{y_1+y_2}\right)\left(\frac{\pi t y_0}{y_1+y_2}\cos\frac{\pi t y_1}{y_1+y_2} - \sin\frac{\pi t y_1}{y_1+y_2}\right) \times\left((y+y_0)\cos\frac{\pi t(y+y_1)}{y_1+y_2} - \frac{y_1+y_2}{\pi t}\sin\frac{\pi t(y_2+y_1)}{y_1+y_2}\right)\right\}. \tag{8.6}$$

To these velocity components must be added the convective velocity component u_c, given by (4.13), which requires numerical integration.

At values of $(x^2+z^2)^{\frac{1}{2}}$ which are not large enough for the expansions to converge satisfactorily, the velocity components due to the nearest regions in the ys-plane may be calculated directly, and the source distribution in more distant regions may be replaced by a smoothed-out source of constant strength in the s-direction.

The bounded shear flows treated in this paper are only samples of the many types which may be successfully studied by use of the method of images. The techniques developed here and simple extensions of them lead to useful quantitative results in many other cases of interest, but the number of possible configurations is so large that there seems little point in attempting to compile a comprehensive list of solutions.

REFERENCES

Courant, R. & Hilbert, D. 1937 *Methoden der mathematischen Physik*, II. Berlin: Springer.

Darwin, C. G. 1953 *Proc. Camb. Phil. Soc.* **49**, 342.

Lighthill, M. J. 1956 *J. Fluid Mech.* **1**, 31.

Lighthill, M. J. 1957*a* *J. Fluid Mech.* **2**, 311.

Lighthill, M. J. 1957*b* *J. Fluid Mech.* **2**, 493.

Lighthill, M. J. 1957*c* *J. Fluid Mech.* **3**, 113.

Olver, F. W. J. 1949 *Quart. J. Mech. Appl. Math.* **2**, 452.

Reuter, G. E. H. 1949 *Quart. J. Mech. Appl. Math.* **2**, 457.